



Bunsho Ohtani

Contents

12.1 Photoacoustic Spectroscopy: Its Principle and Characteristics	303
12.2 Instrumental Setups and Conditions for Photoacoustic Spectroscopy	305
12.3 Single-Beam Photoacoustic Spectroscopic Measurement of Titania Photocatalyst Samples	305
12.4 Double-Beam Photoacoustic Spectroscopy for Titania Photocatalyst Samples	306
12.5 Reversed Double-Beam Photoacoustic Spectroscopy for Titania Photocatalyst Samples	309
12.6 ERDT/CBB Patterns as a Fingerprint of Metal-Oxide Samples	311
12.7 Photoacoustic Spectroscopy as Useful Tool for Solid Materials: Conclusive Remarks	312
References	312

Abstract

Photoacoustic spectroscopy (PAS) is a technique to measure photoabsorption by measuring the intensity of sound generated by the photoabsorption of chopped or modulated, i.e., continual light by a sample, but not by measuring the intensity of light reduced by the sample photoabsorption as is in the ordinary photoabsorption spectroscopy. Therefore, PAS is one of the best techniques or even only sole one to measure photoabsorption by solid materials such as particulate photocatalysts. Another feature of PAS is that photoirradiation of continuous light, even at the same wavelength of continual light for PA signal detection, does not give any influence on the

photoabsorption measurement. This enabled to develop double-beam photoacoustic spectroscopy (DB-PAS), in which two beams, wavelength-scanned modulated light and continuous light which induces photoinduced reaction or change of solid materials, are irradiated to a sample and photoinduced change in photoabsorption of a system. In reversed double-beam photoacoustic spectroscopy (RDB-PAS), wavelength-scanned continuous light and monochromatic continual light are irradiated to follow the change in photoabsorption at the wavelength of continual light induced by wavelength dependent photoinduced reaction.

Keywords

Photoacoustic spectroscopy · PAS · Double-beam photoacoustic spectroscopy · DB-PAS · Reversed double-beam photoacoustic spectroscopy · RDB-PAS · Energy-resolved distribution of electron traps · ERDT · Identification of metal-oxide powders · Degree of coincidence of ERDT patterns

12.1 Photoacoustic Spectroscopy: Its Principle and Characteristics

Photoacoustic (PA) spectroscopy is a kind of techniques to measure photoabsorption by detecting sound generated by continual photoabsorption of substances in any form, solid, liquid, or gas. In PA spectroscopy, after a substance absorbs light (or simply electromagnetic wave), i.e., be excited electronically, vibrationally, or rotationally by UV-visible light, infrared light and microwave, respectively, the resultant excited state releases energy to go back to the original ground state. Since it can be assumed that the excitation energy is, at least partly, released as heat, the substance itself is heated to result in its volumetric expansion. When the irradiated light is modulated (or chopped), a substance is heated continually

B. Ohtani (✉)
Institute for Catalysis, Hokkaido University, Sapporo, Japan
e-mail: ohtani@cat.hokudai.ac.jp

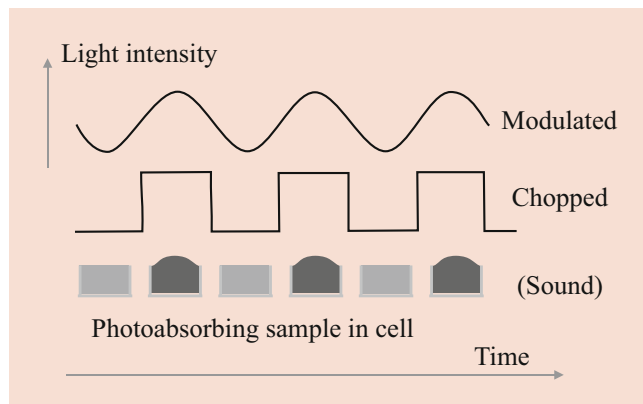


Fig. 12.1 Schematic representation of photoacoustic spectroscopy using modulated (upper) or chopped (lower) light for photoabsorbing sample in a cell

and undergoes expansion-shrinkage cycles to generate sound of frequency same as that of light modulation, which can be detected by a microphone as schematically shown in Fig. 12.1.

The principle of this PA spectroscopy has been reported for the first time by Bell, Alexander Graham Bell, the inventor of telephone, in the late nineteenth century [1] and later several groups used this technique for measurement of photoabsorption of materials [2, 3]. One of the characteristics of this technique is that even solid (powder) materials can be measured without modifications of original procedure and setups for those solid samples, which is highly beneficial considering the limitation of below-mentioned conventional photoabsorption spectroscopy.

In the ordinary (conventional) photoabsorption spectroscopy, intensity of incident light attenuated by a sample (I) is measured to evaluate the extent of absorption by comparison with the original incident-light intensity (I_0) as, absorption (or extinction) = $1 - I / I_0$ as shown in Fig. 12.2. This procedure can be applied to transparent, i.e., non-reflective and non-diffusive (light-scattering), samples. However, for the solid samples, there must be at least two problems. One is the necessity of collection of all reflected and/or scattered light by using, e.g., an integration sphere on the assumption that the inner surface of an integration sphere does not absorb light at all, and all the gathered light is introduced to a detector without loss. The other problem is lack of a standard which should reflect/scatter all the incident light without any absorption, and again a given de-facto standard must be used on the same assumption of no light absorption. Another problem, commonly exists in the ordinary photoabsorption spectroscopy, is that the extent of absorption must be calculated by subtraction, $I_0 - I$, the accuracy of which depends strongly on the detection error of a used detector, and therefore the sensitivity for low absorption cannot be high. On the other hand, PA signal is generated only when a sample

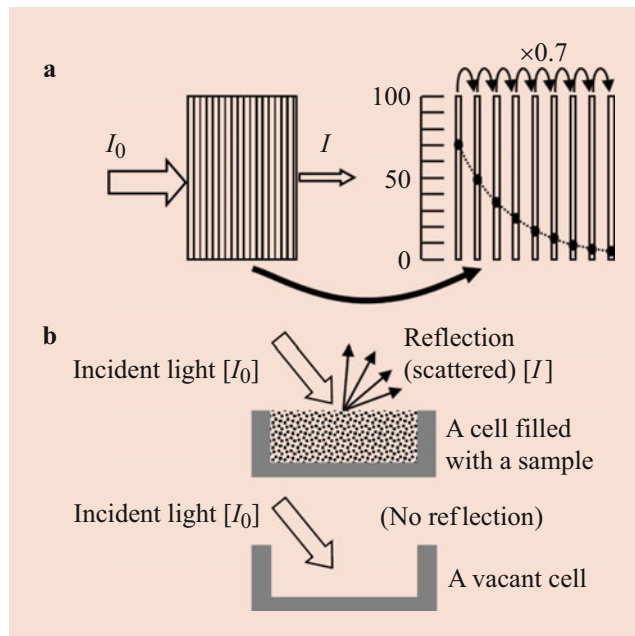


Fig. 12.2 Schematic representation of ordinary photoabsorption spectroscopy in (a) transmission and (b) diffuse reflectance modes. (a) Logarithmic decrease in light intensity by absorption at constant (e.g., 30%) absorption at each thin layer. (b) Extinction (absorption and scattering) measurement for solid samples requires a standard sample which reflects incident light [4]

absorbs light even if incident light is scattered or reflected, and thereby relatively high sensitivity is expected for PA spectroscopy even if highly scattering sample, e.g., powder samples, is used without any pretreatment. Another advantage of PA spectroscopy compared with the conventional spectroscopy is flexibility of wavelength region for measurement; it is unnecessary to choose an appropriate detector depending on the wavelength region, i.e., the detector is always a microphone not depending on the range of light (electromagnetic wave), e.g., microwave, infrared, visible, or UV-range photoabsorption measurements.

Only one possible disadvantage of PA spectroscopy, the present author thinks, is that PA measurement gives only relative extent of photoabsorption. How much absolute extent of incident light is absorbed cannot be obtained, though detected PA intensity as sound can be assumed, in principle, to be proportional to extent of absorption of incident light, absorption ($I_0 - I$) which is measured in conventional spectroscopy, i.e.,

$$\begin{aligned} & \text{(PA signal intensity (arbitrary unit))} \\ & = f(x, y, z, \dots) (I_0 - I). \end{aligned} \quad (12.1)$$

Possible parameters included in a function f are photoabsorption coefficient, incident-light intensity (I), efficiency of heat release upon deexcitation, heat capacity and heat

transfer rate of a sample, frequency of light-intensity modulation, density (gas phase between a sample and a microphone), viscosity of a medium and temperature of a medium, sensitivity of a microphone, and magnitude of amplification of signal in lock-in detection, but not limited to these parameters. For the compensation of light-intensity change, carbon black is frequently used as a standard for visible light-range PAS measurement by assuming complete absorption of incident light. Compared to the assumption of 100% reflection in the diffuse-reflectance measurement, this assumption is highly probable.

12.2 Instrumental Setups and Conditions for Photoacoustic Spectroscopy

A schematic representation of conventional PAS setup is shown in Fig. 12.3. The setup is composed of (i) light source, (ii) monochromator, (iii) light chopper, (iv) cell equipped with a microphone, (v) function generator, and (vi) lock-in amplifier. Light chopper (iii) is a device with rotating plates with holes to chop light beam, i.e., modulates light intensity of light from a light source (i) monochromatized by a monochromator (ii) in nearly rectangular wave. In principle, if the output of a power source for a light source (i), e.g., xenon arc lamps, can be modulated, a light chopper is unnecessary, though the present author does not know such modulation for xenon or mercury arc lamps. A function generator (v) provides modulated signal (or output) to a chopper (iii) as well as a lock-in amplifier (vi) as a reference. A PA cell (iv) is equipped with a window through which a modulated-light beam is introduced into closed space and a microphone which provides a signal. This type of PAS cell has been originally designed and reported by Toyoda's group [5–7]. A signal (sound) synchronized with the modulated

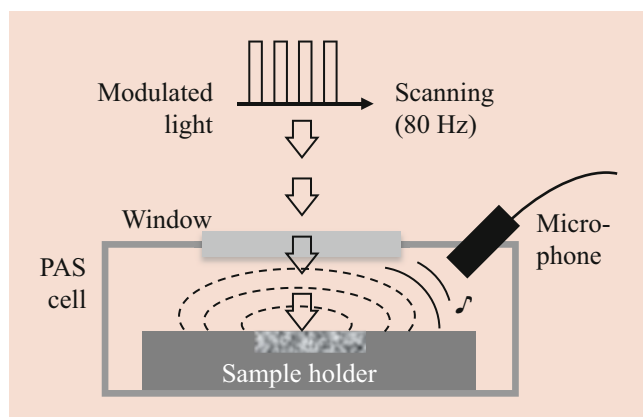


Fig. 12.3 A schematic representation of conventional photoacoustic spectroscopy setup

light, i.e., of frequency same as that modulated light, from a microphone is detected using a lock-in amplifier (vi).

As pointed out in Sect. 12.1, PA spectroscopy has, in principle, no limitation of wavelength of light if the created sound of light intensity-modulation frequency can be detected by a microphone in a PA cell. In practice, visible to ultraviolet (ca. 250–800 nm) or infrared ($800\text{--}4000\text{ cm}^{-1}$) light is used. For the quality of monochromatic light depending on the width of slits equipped on a monochromator; the higher the intensity by opening slits is, the higher becomes detected PA signal intensity, while the lower becomes wavelength accuracy of obtained PA spectra. When a PA spectrum is to be compared with that recorded on an ordinary spectrometer, in which wavelength accuracy is lower than 1 nm, slits on a monochromator should be rather closed. However, photoabsorption of solid materials is generally structureless, i.e., no sharp peaks are included, and high wavelength accuracy is unnecessary. Compared with the above-mentioned parameters, selection of modulation (chopping) frequency is highly important. For example, PA signal intensity is significantly changed by modulation frequency. It is also known that measured depth from the sample surface is influenced by the frequency. Those frequency effects may appear depending on the PA measurement conditions, modulated-light wavelength, samples or a medium between a sample and a microphone. Therefore, the best condition must be determined by trial-and-error ways. Fortunately, in the ordinary setups, modulation frequency is controlled by a function generator and frequency can be flexibly changed.

12.3 Single-Beam Photoacoustic Spectroscopic Measurement of Titania Photocatalyst Samples

Results of single-beam (SB) PAS measurement of several commercial titanium (IV) oxide powder samples by the author's group are shown in Fig. 12.4a [8, 9]. In the measurements, samples in a closed cell was irradiated under ambient air atmosphere with wavelength-scanned monochromatic light extracted from the output of a 300-W Xenon lamp using a grating-type monochromator and modulated by a light chopper at 80 Hz. The PA signal was acquired by an electret condenser microphone (ECM) buried in the cell, amplified/monitored by a digital lock-in amplifier and normalized (plotted in arbitrary unit) using a carbon black powder as a reference to compensate wavelength-dependent light intensity. For most of the titania samples, when the irradiation light intensity was enough low, repeated SB-PAS measurements did not cause any notable change in the spectra. The detected and plotted PA signal corresponds to generation of heat as a result of relaxation of photoexcited states,

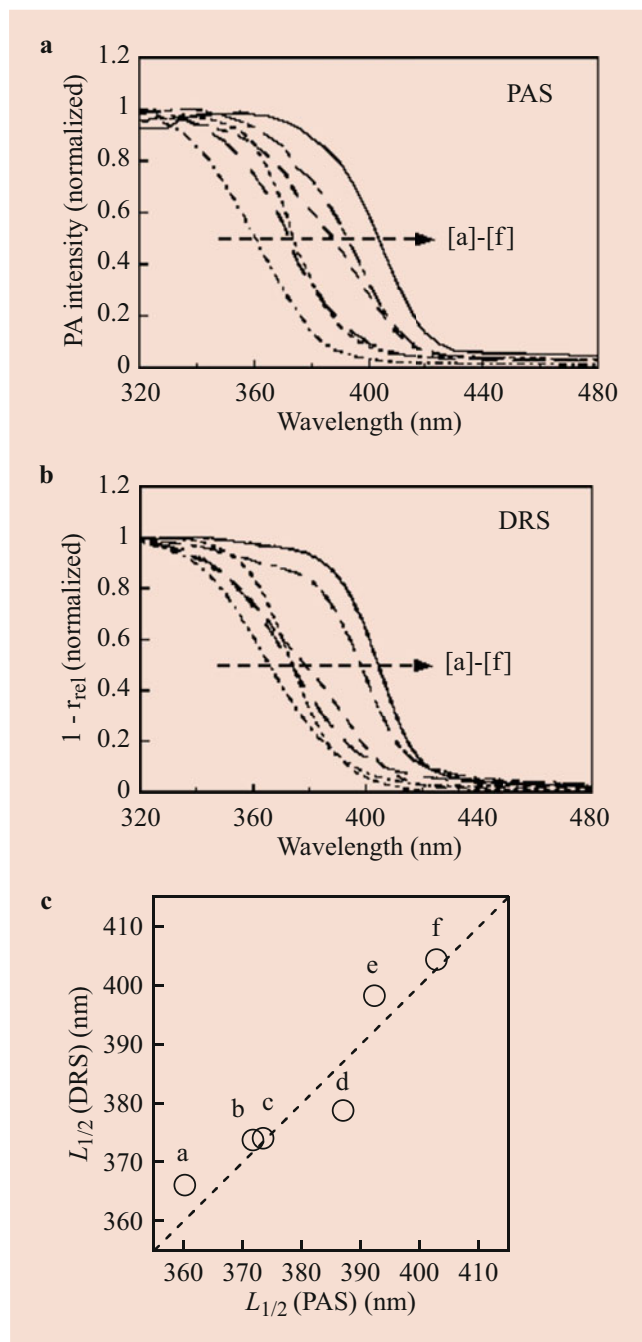


Fig. 12.4 (a) SB-PA and (b) diffuse reflectance spectra normalized at maximum value of (curve a) Wako {amorphous}, (curve b) JRC-TIO-12 {A}, (curve c) Merck {A}, (curve d) Degussa P25 {A/R}, (curve e) JRC-TIO-6 {R}, and (curve f) CR-EL {R/A}. A and R in braces denote the predominant crystal phase, anatase or rutile. Measurements were performed in the ambient air. (c) Relation between $L_{1/2}$ for PAS and for DRS. (Originally Fig. 1 in [8])

i.e., recombination of photoexcited electron-positive hole pairs in the above-band gap wavelength ($<$ ca. 400 nm) region. The heat generated by their recombination is expected to be proportional to photoabsorption, since photoluminescence from photoexcited pristine titania is negligible

at ambient temperature and chemical reaction by photoexcited electrons and positive holes might be slow and independent of wavelength.

In order to be compared with the SB-PA spectra, ordinary photoabsorption spectra were recorded on a photonic multi-channel analyzer in diffuse reflectance (DR) mode as shown in Fig. 12.4b for those titania samples, in which absorption ($1 - r_{\text{rel}}$, where r_{rel} is diffuse reflectance of a sample relative to that of a barium sulfate (BaSO_4) standard) was plotted against wavelength. Those DR spectra showed reasonable resemblance with SB-PAS spectra shown in Fig. 12.4a since both PA and DR spectra correspond to wavelength dependence of photoabsorption of samples. Both PA and DR spectra showed saturation at a shorter wavelength. The saturation wavelength was dependent on the sample, but the order of shift in the onset wavelength of each titania sample seemed the same. In order to compare those two kinds of spectra, the wavelength giving half intensity of saturation, $L_{1/2}$ was calculated as a tentative measure of the shift in these spectra and was plotted in Fig. 12.4c. As is clearly seen, an almost linear relation was observed, and this indicated that these two kinds of spectra are reflected by the same phenomenon, i.e., photoabsorption.

Depending on the crystal structure of titania samples, rutile, anatase, and amorphous, onset wavelengths were shifted from ca. 420 to ca. 380 nm in both PA and DR spectra, reflecting the bandgaps of 3.0 eV, 3.2 eV and larger, respectively. The spectrum of anatase-rutile mixed Evonik (previously Degussa) P25 (Fig. 12.4d) showed an intermediate character between those of single-phase rutile and anatase samples. Even though both JRC-TIO-6 and CR-EL are rutile (CR-EL contains a small percentage of anatase), an appreciable spectral difference between JRC-TIO-6 and CR-EL was observed, probably due to the difference in their primary particle sizes, ca. 15 nm and ca. 200 nm, respectively. Those features appeared similarly in both SB-PA and DR spectra, indicating that PA spectra can be used similarly to ordinary DR spectra.

12.4 Double-Beam Photoacoustic Spectroscopy for Titania Photocatalyst Samples

As has been described in the preceding sections, PA signal is created by continual photoabsorption due to intensity modulation of irradiated light, which means that continuous light irradiation does not give any influence on the PA measurement. Therefore, even if continuous light of the wavelength identical to that of modulated/chopped light for PA-signal acquisition is irradiated to and absorbed by a sample, PA measurement itself is not affected. When the overlapped continuous light induces structural change to result in

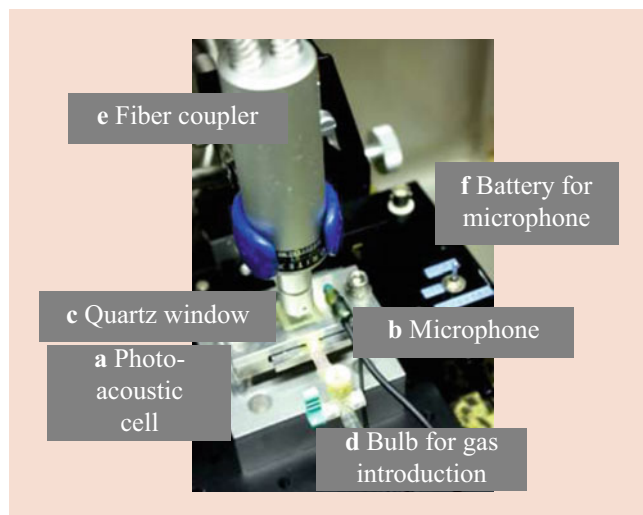


Fig. 12.5 A photo of a part of double-beam photoacoustic measurement setup. (a) photoacoustic cell, (b) buried electret condenser microphone, (c) quartz window, (d) bulbs for gas introduction, (e) fiber coupler, and (f) battery for microphone

photoabsorption-property change in a sample, PA signal follows such change. Although PA spectroscopy using continual and continuous light beams, or simply PA measurement under continuous-light irradiation might have been reported before the publication by the present author's group, a term "double-beam photoacoustic spectroscopy" was used for the first time in our paper [8, 9].

Setup for double-beam photoacoustic spectroscopy (DB-PAS) is built simply by combining a continuous-light beam to modulated (chopped) light beam. For this purpose, the author's group use a fiber coupler which combine two beams into one as is shown in Fig. 12.5. For continuous light source, polychromatic or monochromatic light can be used.

The commercial titania samples were used again in the DB-PAS measurements. They were categorized into two groups, type-1 and type-2 on the basis of spectral behavior observed in DB-PAS measurements. The first type-1-group samples showed an upward shift of the PA spectrum at >380 nm under simultaneous continuous UV irradiation, i.e., DB-PAS measurement in ambient air conditions. The upward-shifted almost flat spectrum was recovered to the original spectrum in the dark after the measurement as shown in Fig. 12.6 for JRC-TIO-11 sample. Visible light of wavelength at >450 nm instead of continuous UV light induced no such upward shift in the DB measurements, indicating that the upward shift was caused by bandgap excitation of titania. Since purging of ambient air by dry nitrogen before the measurement enhanced the upward shift and reduced the rate of recovery (color fading) in the dark, suggesting that accumulation of photoexcited electrons, which are possibly consumed by surface-adsorbed oxygen as an electron acceptor, is attributable to the PA spectral shift

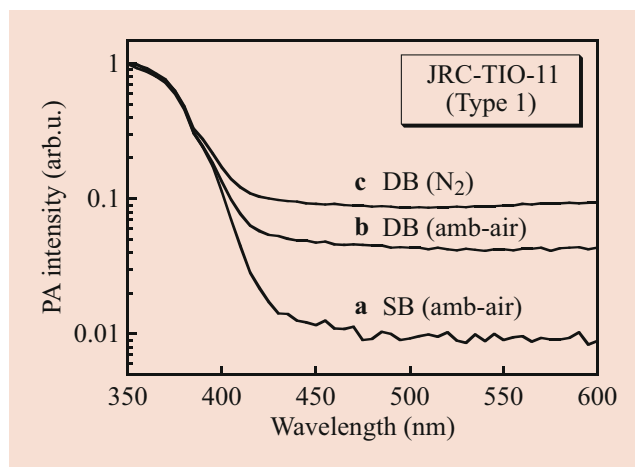


Fig. 12.6 PA spectra of JRC-TIO-11. (Curve a) SB spectrum measured in ambient air. Final-state spectrum by repetition of DB measurements (curve b) in ambient air and (curve c) under N_2 [8]

in the visible region. Another possible reason for difference in DB-PA spectra under ambient air and dry nitrogen is humidity in ambient air, but the fact that there was no appreciable difference in DB-PA spectra taken under ambient air and artificial air, mixture of dry nitrogen and oxygen revealed that influence of humidity in ambient air on DB-PA spectra could be neglected.

The above-mentioned upward shift of spectra of type-1 samples in DB-PAS measurements is accounted for by titanium(III) (Ti^{3+})-species liberation under UV irradiation as a counterpart of hole consumption presumably by residual organic compounds adsorbed on the surface, as the presence of such impurities acting as electron donors in titania samples stored under ambient atmosphere has been proved. It has often been observed the carbon-dioxide liberation from UV-irradiated aqueous titania suspensions in the absence of any additives under aerobic conditions and change of color from white to gray of UV-irradiated titania suspensions under deaerated conditions. These observations were interpreted by the presence of electron-donating carbon-containing compounds and accumulation of electrons in electron traps (ETs) in the absence of oxygen as a scavenger of photoexcited and/or trapped electrons. Such Ti^{3+} accumulation in titania samples has also been reported for titanias under UV irradiation [10–12] or anodic polarization [13]. Thus, electron accumulation, i.e., trapping by ETs, proceeded for type-1 titania samples in DB-PAS measurement. Therefore, it was also reasonable to find that the upward shift was enhanced by the presence of hole scavengers such as methanol vapor because electron accumulation is promoted by effective hole consumption.

Among several type-1 samples, JRC-TIO-6 showed a little different behavior in DB-PAS measurement. Although most of the type-1 samples showed similar almost flat upward shifts regardless of their chemical and physical properties,

JRC-TIO-6 showed slightly different spectral behavior under aerobic or partly aerobic conditions, i.e., its DB-PA spectra taken under artificial-air conditions was almost the same as the original PA spectrum, and upward shift, slightly higher at a shorter wavelength range (450–500 nm), was observed when air was diluted three times by argon, while under deaerated conditions, almost flat upward shift was observed. These facts suggest that JRC-TIO-6 has higher sensitivity to oxygen, which retards accumulation of Ti^{3+} to give visible-light photoabsorption, than those of the other type-1 samples, probably due to its relatively high specific surface area (ca. $100 \text{ m}^2 \text{ g}^{-1}$) to hold large amount of oxygen on the surface.

The second type-2 group samples were composed of anatase, without rutile crystallites, with relatively high specific surface area ($>250 \text{ m}^2 \text{ g}^{-1}$), including, e.g., Hombikat UV-100, JRC-TIO-7–10 or 12. SB- and DB-PA spectra of JRC-TIO-12 as a representative type-2 sample is shown in Fig. 12.7. General trends of type-2 samples were (a) PA signal increase at 380–500 nm in repeated SB measurements under aerobic conditions, but not under deaerated conditions, (b) this band was also observed in subsequent DB-PAS measurements and (c) the band was decreased in repeated DB-PAS measurements to give finally a type-1-like flat shift observed under deaerated conditions. Since the 380–500-nm band was grown during UV-wavelength ($<400 \text{ nm}$) scanning in SB-PAS measurement, this PA signal was originated from bandgap excitation in the presence of oxygen, i.e., the type-2 samples were shown to be sensitive to ambient oxygen rather than the type-1 samples and to give PA band at 380–500 nm. An amorphous titania sample (Wako Pure Chemical) also showed this 380–500 nm band mainly in subsequent DB-PAS measurements, but not in the preceding SB-PAS measurement. Since the bandgap of amorphous titania is estimated to be larger than

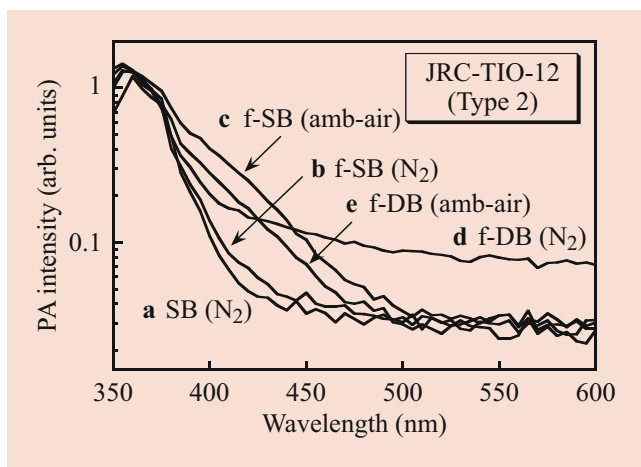


Fig. 12.7 PA spectra of JRC-TIO-12. (Curve a) Initial-state spectrum by SB measurement under N_2 , final-state spectrum by repetition of SB measurements (curve b) under N_2 and (curve c) in ambient air, final-state spectrum by repetition of DB measurements (curve d) under N_2 and (curve e) in ambient air [8]

that of anatase titania, i.e., amorphous titania absorbs light of shorter wavelength compared with anatase, the observed slow rate of the 380–500 nm band appearance in repeated SB-PAS measurements is attributable to a smaller number of photons absorbed during SB-PAS measurements.

For the assignment of the 380–500-nm band, there seem to be two possibilities. One is photoabsorption of trapped holes, which were produced by stabilization of positive holes in certain states after electron transfer to an acceptor, such as oxygen, on the titania surface. This was supported by the fact that oxygen as an acceptor and methanol as a donor in the PAS cell enhanced and reduce the band appearance, respectively. It has been reported that similar transient absorption peak at ca. 430 nm was observed in time-resolved spectroscopic studies on titania samples in the presence of electron scavengers [14], while different results were also observed in the other studies [12, 15] as these peaks and shapes of spectra were much sensitive to surface conditions and kinds of electron donors/acceptors [12]. It has been elucidated that the lifetime of these trapped holes was much shorter than that of the present study.

Another possible assignment of the 380–500-nm band is surface peroxy species. This is supported by the reports claiming that similar 350–500-nm band appeared by treatment of titania samples with aqueous hydrogen peroxide [16–19]. It has been reported [18] that hydrogen-peroxide treatment of type-1 samples, JRC-TIO-3 and JRC-TIO-5, induced the development of photoabsorption at 380–500 nm. It should be noted that for these type-1 samples such absorption could not be observed in the DB-PAS measurements, suggesting that type-1 samples produce less amount of hydrogen peroxide by bandgap excitation. The 380–500-nm photoabsorption was actually observed for a hydrogen peroxide-treated type-2 sample, JRC-TIO-12, in its SB-PA spectrum, and the band disappeared to give flat spectral shift by subsequent repeated DB-PAS measurement, as shown in Fig. 12.8. Thus, it is type-2 titania samples produce appreciable amount of surface-adsorbed hydrogen peroxide and/or surface peroxy species by UV-irradiation (bandgap excitation) in the presence of surface-adsorbed oxygen, which captures a photoexcited electron. Liberation of such peroxy species on photoirradiated titania samples in the presence of oxygen has been suggested [20, 21]. Although an alternative hydrogen peroxide-formation mechanism by coupling of hydroxyl radicals, i.e., through positive hole-oxidation processes, is assumed, the fact that PA increase was negligibly observed by repetition of the SB-PAS measurements under nitrogen where hydroxyl radical-coupling reaction may proceed suggested the exclusion of hydroxyl radical-coupling mechanism. Another mechanism of direct formation of titanium peroxy species through the mechanism not including oxygen, hydrogen peroxide, or hydroxyl radicals has been proposed [22]. However, those mechanism not including oxygen as a source of the peroxy species seems inconsistent

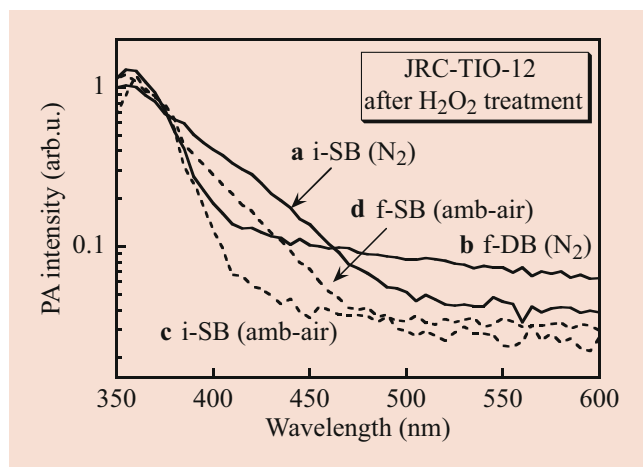


Fig. 12.8 PA spectra of JRC-TIO-12 after H_2O_2 treatment. (Curve a) Initial-state SB and (curve b) final-state DB spectrum under N_2 . (Curve c) Initial-state SB and (curve d) final-state SB spectrum of untreated sample under ambient air [8]

with the fact that the 380–500-nm photoabsorption disappeared by subsequent repeated DB-PAS measurement to be changed to flat shift (Ti^{3+} accumulation) of PA spectra.

Thus, DB-PA spectroscopy has revealed that titania samples undergo reduction to accumulate Ti^{3+} species, trapped electrons, under continuous UV irradiation, as well as surface peroxy species (surface-adsorbed hydrogen peroxide) for type-2 samples owing to contaminated oxygen on their surface. The latter process could be neglected when enough amount of electron donors to consume oxygen almost entirely during DB-PAS measurements, and therefore almost all the ETs seemed to be filled up by relatively long-time DB-PAS measurements under methanol-saturated nitrogen atmosphere. Figure 12.9 shows the relation between saturated PA intensity in DB-PAS measurements and amount of Ti^{3+} evaluated by previously reported photochemical method in which ETs in a sample is filled up by photoirradiation in the presence of electron donors followed by electron transfer to methyl viologen in a suspension [23]. When methanol-saturated nitrogen was used, almost linear relation was between them, suggesting that DB-PAS enables the evaluation of total density of ETs in a sample and its absolute amount can be determined by a calibration curve in the figure for, at least, titania samples.

12.5 Reversed Double-Beam Photoacoustic Spectroscopy for Titania Photocatalyst Samples

As described in the preceding sections, PAS can show the photoabsorption of solid materials such as photocatalyst powders or thin films, and DB-PAS can detect the photoinduced change in photoabsorption of solid materials. In

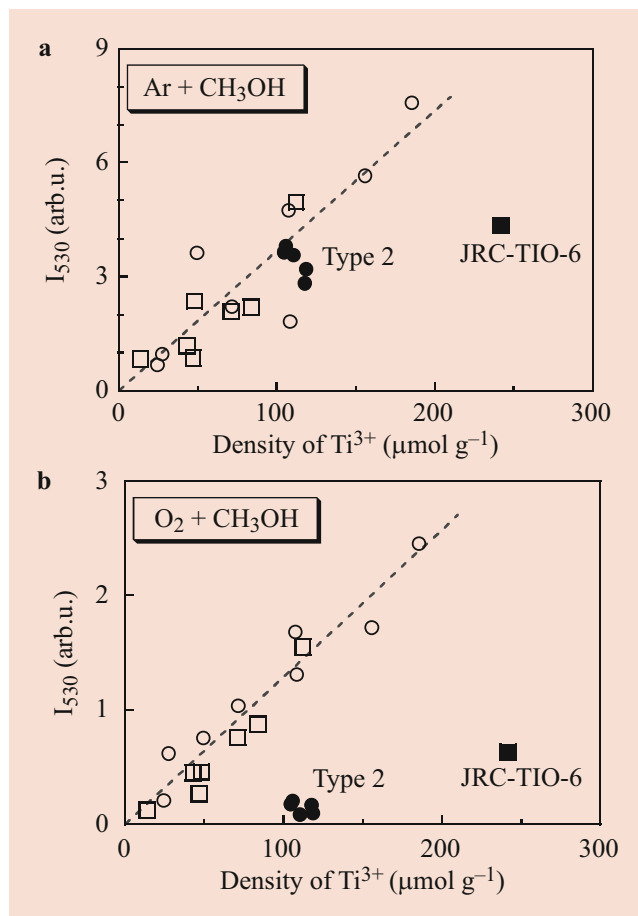


Fig. 12.9 Relation between the saturation limit of PA intensity (I_{530}) under (a) $\text{Ar} + \text{CH}_3\text{OH}$ and (b) $\text{O}_2 + \text{CH}_3\text{OH}$ and density of Ti^{3+} . Predominantly anatase (\circ), predominantly rutile (\square), type-2 sample (\bullet), JRC-TIO-6 (\blacksquare). Numbers “1” and “2” in panel (a) show I_{530} in repeated experiments which were operated to check the reproducibility [8]

principle, any change in photoabsorption can be detected by DB-PAS, and one of the examples is detection of photoabsorption by trapping photoexcited electrons and/or positive holes by bandgap excitation of photocatalyst powders as described above. In those measurement, the continuous (relatively intense) light creates photoexcited electrons and positive holes, which are then trapped in certain electron/hole trapping sites, and the modulated (chopped) light is used for PA detection of photoabsorption due to trapped electrons/holes. As a result, photoabsorption spectra of photoreaction products is obtained by DB-PAS.

The electron traps (ETs) in titania photocatalyst powders have been characterized before our publication on DB-PAS. Total ET density, measured in the unit of $\mu\text{mol g}^{-1}$, of several commercial titania samples was estimated by photochemical method using methyl viologen as an electron acceptor [23], and DB-PAS could also be used for this total ET density as described above. In the measurement procedure, an aqueous suspension of a titania sample was UV photoirradiated in the

presence of electron donors such as methanol or triethanolamine to make photoexcited electrons trapped in ETs. In the photochemical method, it was also possible to measure energy-resolved distribution of ETs (ERDT) by controlling pH of a reaction mixture before electron transfer from ETs to methyl-viologen molecules [23]. As an ERDT-measurement technique, the photochemical method using methyl viologen has at least three problems; (1) tedious procedure of pH titration under deaerated conditions, e.g., in a glove box, (2) low resolution of energy of ETs due to the limitation of precise pH control, and (3) limited energy range since maximally 0–14 in the pH unit. Consequently, direct measurement of photoabsorption by accumulation of electrons in ETs, like DB-PAS, seems useful for ERDT measurement. Although bandgap excitation is also used in DB-PAS, accumulation of electron occurs randomly not depending on the energy of ETs and thereby ERDT cannot be measured in such operation mode.

Reversed double-beam photoacoustic spectroscopy (RDB-PAS) has then been developed to measure ERDT of photocatalyst powder samples, in which a continuous light is wavelength scanned and a modulated light is wavelength fixed, reversed to DB-PAS [24, 25]. Practical setup of the original RDB-PA spectroscopy is shown in Fig. 12.10. The measurement was performed under methanol-saturated nitrogen which was introduced in a cell containing a powder sample-loaded holder by passing through it prior to measurement. Methanol was chosen as a sole possible gaseous positive-hole scavenger, which is used to avoid once accumulated electrons in ETs react with positive holes left in VB and able to be introduced in the cell. A UV quartz combiner light guide (Moritex MWS5-1000S-UV3) was used to introduce two light beams for pump and probe into the cell. The pump beam was continuous monochromatic light from the xenon lamp-monochromator (a Spectral Products CM110 1/8 m grating monochromator with a Spectral Products ASB-XE-175 xenon light source, same as those used in conventional PAS and the above-mentioned DB-PAS measurements shown in Fig. 12.1) and the probe beam was intensity-modulated (80 Hz by an NF Corporation DF-1906 digital function generator) light-emitting diode (LED) light (Luxeon LXHL-ND98). RDB-PA spectra were recorded by scanning the pump-beam wavelength from 650 nm to 350 (or 300 nm) with a 5-nm step, detecting PA signal with 255-s waiting and 20-s acquisition times as a standard, and plotting as a function of energy of pump light. Density of ETs was calculated by differentiation of an obtained RDB-PA spectrum and converted to that shown in the unit of $\mu\text{mol g}^{-1} \text{eV}^{-1}$ (the part eV^{-1} was introduced to make integration of bars) using conversion coefficients for each set of a measurement cell and a probe LED light with reference to the results of chemical-titration ET-density

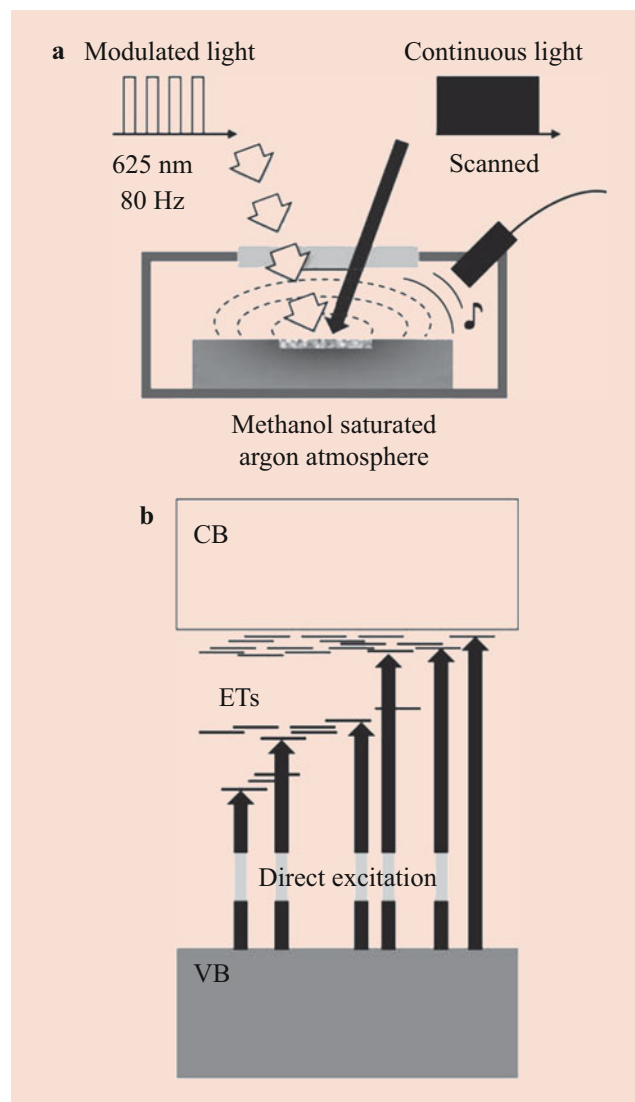


Fig. 12.10 (a) Schematic diagram and (b) principle of RDB-PAS measurement [25]

measurement [23] and plotted as a function of energy from valence-band top (VBT), in convenience, as a bar graph with 0.05-eV pitch [24, 25].

Figure 12.11 shows the representative result of RDB-PAS measurements. As depicted in Fig. 12.11b, PA-signal intensity corresponding to the photoabsorption of a sample at 625 nm was first gradually and then steeply increased and was then saturated at ca. 350 nm during the course of scanning of the pump-light wavelength, reflecting the accumulation of electrons from the low-energy (deeper) side to the higher-energy (shallower) side and increase in photoabsorption in the 450–650-nm visible-light wavelength range as had been observed in the above-mentioned DB-PAS. Saturation of the PA-signal intensity at the end of pump light-wavelength scanning (350 nm) was commonly observed for titania samples suggesting that all ETs in this

sample having energy lower than ca. 3.5 eV, which is a little higher than the conduction-band bottom (CBB; ca. 3.2 eV), were filled up under the appropriate measurement conditions with a sufficiently long waiting time, and electrons cannot be accumulated in the conduction band. This RDB-PA spectrum (Fig. 12.11b) is an integrated form of energy distribution of ETs (ERDT) and, therefore, an ERDT pattern can be obtained by differentiation of an RDB-PA spectrum from the lower energy (longer wavelength) side as shown in Fig. 12.11c as a function of energy from VBT, in which absolute ET density is shown in the unit of $\mu\text{mol g}^{-1} \text{eV}^{-1}$ as described above. The reason why ETs are located also in the energy-range of CB not limited to that in the bandgap has not yet been clarified. One of the possible reasons is that the electronic transition to ETs occurs not from VBT but a high DOS (density of states) part of VB because of very low ET density and negligible DOS at VBT. This is supported by the observed 0.1–0.2-eV upward (higher-energy side) shift of ERDT obtained by RDB-PAS compared with that measured by chemical titration [25].

In the RDB-PAS measurement, a 625-nm red LED light was used as a probe beam to avoid possible VB-ET transition by this probe beam and photoabsorption by peroxide species in the ca. 400–500-nm wavelength range. Actually, as is well known, visible-light photoabsorption by titania samples is negligibly small, i.e., below the detection limit of ordinary photoabsorption spectroscopy, indicating that direct detection of VB-ET electronic transition of negligible photoabsorption

coefficient cannot be measured by ordinary photoabsorption spectroscopy. However, the VB-ET photoexcitation can be driven in the actual measurement because the photoabsorption coefficient is not zero and removing positive holes in VB by the VB-ET transition make it possible to accumulate electrons in ETs which are then measured by PAS. If the waiting time, i.e., time for complete filling of ETs at certain energy, is not sufficiently long, the left unfilled ETs are filled at higher-energy pump beam and the corresponding ERDT pattern may be shifted to higher-energy side.

Since the PA signal, i.e., photoabsorption at the probe-light wavelength, is originated from electrons in ETs, accuracy of ERDT patterns can be guaranteed only when ET-filling electrons remain without transfer. In fact, if platinum (Pt)-loaded titania samples were used, almost no increase in PA intensity was observed due to possible efficient electron transfer from electron-filled ETs in titania to Pt to induce hydrogen evolution on the Pt surface; in overall, titania-photocatalyzed methanol dehydrogenation proceeds during the measurement. This also indicates that titania ETs are located predominantly on the surface or within a distance sufficiently short from the surface-deposited Pt. Actually, the total density of ETs of various commercial titania samples were increased along with their specific surface area [24, 25].

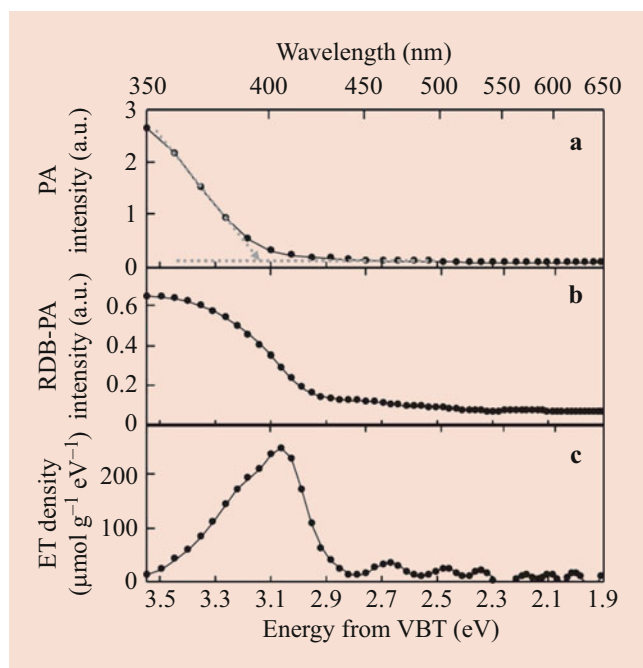


Fig. 12.11 (a) PA spectrum, (b) RDB-PA spectrum, and (c) differentiated spectrum of (b) for a commercially available titania sample (JRC-TIO-1)

12.6 ERDT/CBB Patterns as a Fingerprint of Metal-Oxide Samples

Figure 12.12 shows the representative result of RDB-PAS measurements for commercial titania samples. In those measurements, ordinary PA spectra corresponding to photoabsorption spectra were also obtained using the same PA cell with different photoirradiation mode and bandgap energy

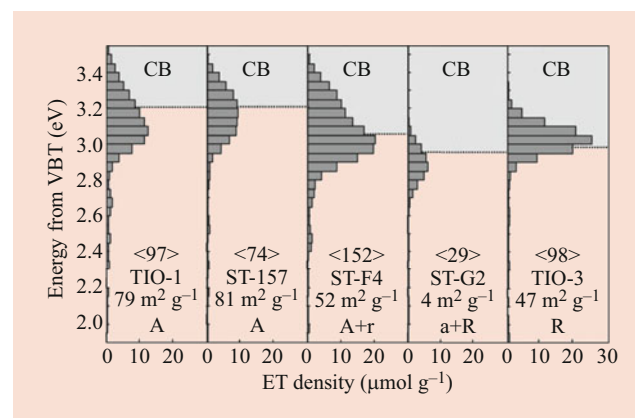


Fig. 12.12 Representative ERDT/CBB patterns of anatase, rutile, and mixed phase titania powders. Each bar shows subtotal ET density in the 0.05-eV energy range [25]

of each sample was calculated from the absorption-edge wavelength. Since bandgap energy is a difference CBB and VBT, the calculated bandgap corresponds to energy of CBB in reference to VBT, and thereby CBB can be shown in an ERDT pattern with the same energy scale. It seemed that the CBB position depends only on the bulk structure, i.e., crystalline phase, of titania samples, anatase, rutile, and the others. This suggests that CBB position may reflect bulk structure of samples. ERDT patterns were, on the other hand, different with each other even if the crystalline phase was the same. As described in the preceding section, the total ET density is increased with specific surface area of samples and thereby the most ETs are located on the surface, suggesting that ERDT pattern and total ET density may reflect surface structure and surface (bulk) size of samples, respectively. Consequently, it is possible to claim that ERDT/CBB patterns can be fingerprints of samples which possess ETs reflecting three fundamental structural properties of solids, bulk structure, surface structure, and surface (bulk) size. Identification of solid materials, especially metal-oxide powders, but not limited to photocatalysts, using their ERDT/CBB patterns as fingerprints has been proposed [24, 26, 27].

12.7 Photoacoustic Spectroscopy as Useful Tool for Solid Materials: Conclusive Remarks

As described above, photoacoustic spectroscopy (PAS) has been used successfully in the studies of photocatalysis as a useful tool to measure photoabsorption by solid photocatalyst materials. PAS and DB-PAS provide spectroscopic features of original photocatalysts and those under bandgap excitation, respectively, i.e., wavelength-dependent photoabsorption. Using those techniques, time-dependent change in photoabsorption [28, 29], total density of ETs [30, 31], and reaction heat [32] have been studied. On the other hand, RDB-PAS gives information on wavelength-dependent photoinduced change in photoabsorption, an action spectrum, by accumulation of electrons in ETs. The group of the present author is developing a novel technique, double-scan double-beam photoacoustic spectroscopy (DS-DB-PAS), i.e., RDB-PAS with wavelength-scanning probe beam to record energy-dependent spectra of electron-filled ETs; both photoabsorption and action spectra are measured at the same time.

In those photoacoustic measurements, laboratory-made instrumental setups have been used, since no commercial products are available. This might be a barrier to prohibit making PAS and PAS-based techniques popular. However, PAS requires no large-scale instruments, but an essentially simple and small devices. The present author hopes the researchers in the field of material sciences, not limited to

that of photocatalysis, use PAS and PAS-based techniques and welcomes collaboration works and technology transfers.

Acknowledgments

The authors thank Professor Taro Toyoda (The University of Electro-Communications) and the staff of the Technical Division of Institute for Catalysis (Hokkaido University) for basic design of PAS setups and construction of the apparatuses, respectively. We are highly grateful to Professor Naoya Muramami (Kyushu Institute of Technology) and Dr. Akio Nitta (Graduate School of Environmental Science) for their contribution toward development of DB-PAS and RDB-PAS, respectively.

References

1. Bell, A.G.: On the production and reproduction of sound by light. *Am. J. Sci.* **20**(118), 305–324 (1880)
2. Rosencwaig, A., Gersho, A.: Theory of the photoacoustic effect with solids. *J. Appl. Phys.* **47**, 64–69 (1976)
3. Tam, A.C.: Applications of photoacoustic sensing techniques. *Rev. Mod. Phys.* **58**, 381–432 (1986)
4. Ohtani, B.: Photocatalysis A to Z—what we know and what we do not know in a scientific sense. *J. Photochem Photobiol C: Photochem Rev.* **11**, 157–178 (2010)
5. Toyoda, T., Shimamoto, S.: Effects of Bi₂O₃ impurities in ceramic ZnO on photoacoustic spectra and current-voltage characteristics. *Jpn. J. Appl. Phys.* **37**, 2827–2831 (1998)
6. Toyoda, T., Kawano, H., Shen, Q., Kotera, A., Ohmori, M.: Characterization of electronic states of TiO₂ powders by photoacoustic spectroscopy. *Jpn. J. Appl. Phys.* **39**, 3160–3163 (2000)
7. Toyoda, T., Tsuboya, I.: Apparent band-gap energies of mixed TiO₂ nanocrystals with anatase and rutile structures characterized with photoacoustic spectroscopy. *Rev. Sci. Instrum.* **74**, 782–784 (2003)
8. Murakami, N., Prieto-Mahaney, O.-O., Abe, R., Torimoto, T., Ohtani, B.: Double-beam photoacoustic spectroscopic studies on transient absorption of titanium(IV) oxide photocatalyst powders. *J. Phys. Chem. C.* **111**(32), 11927–11935 (2007)
9. Murakami, N., Prieto-Mahaney, O.-O., Torimoto, T., Ohtani, B.: Photoacoustic spectroscopic analysis of photoinduced change in absorption of titanium(IV) oxide photocatalyst powders: a novel feasible technique for measurement of defect density. *Chem. Phys. Lett.* **426**(1–3), 204–208 (2006)
10. Shultz, A.N., Jang, W.J., Hetherington III, W.M., Baer, D.R., Wang, L., Engelhard, M.H.: Comparative second harmonic generation and X-ray photoelectron spectroscopy studies of the UV creation and O₂ healing of Ti³⁺ defects on (110) rutile TiO₂ surfaces. *Surf. Sci.* **339**, 114–124 (1995)
11. Highfield, J.G., Grätzel, M.: Discovery of reversible photochromism in titanium dioxide using photoacoustic spectroscopy. Implications for the investigation of light-induced charge-separation and surface redox processes in titanium dioxide. *J. Phys. Chem.* **92**, 464–467 (1988)
12. Yoshihara, T., Katoh, R., Furube, A., Tamaki, Y., Murai, M., Hara, K., Murata, S., Arakawa, H., Tachiya, M.: Identification of reactive species in photoexcited nanocrystalline TiO₂ films by wide-wavelength-range (400–2500 nm) transient absorption spectroscopy. *J. Phys. Chem. B.* **108**, 3817–3823 (2004)
13. Toyoda, T., Hayashi, M., Shen, Q.: Photoacoustic and photoelectrochemical current response of nanostructured TiO₂ electrodes. *Jpn. J. Appl. Phys.* **42**, 3036–3040 (2003)
14. Bahnemann, D., Henglein, A., Spanhel, L.: Detection of the intermediates of colloidal TiO₂-catalysed photoreactions. *Faraday Discuss. Chem. Soc.* **78**, 151–163 (1984)

15. Bahnemann, D., Henglein, A., Lili, J., Spanhel, L.: Flash photolysis observation of the absorption spectra of trapped positive holes and electrons in colloidal titanium dioxide. *J. Phys. Chem.* **88**, 709–711 (1984)
16. Boonstra, A.H., Mutsaers, C.A.H.A.: Adsorption of hydrogen peroxide on the surface of titanium dioxide. *J. Phys. Chem.* **79**, 1940–1943 (1975)
17. Munuera, G., Gonzalez-Elipe, A.R., Fernandez, A., Malet, P., Espinos, J.P.: Spectroscopic characterisation and photochemical behaviour of a titanium hydroxyperoxo compound. *J. Chem. Soc., Faraday Trans. 1.* **85**, 1279–1290 (1989)
18. Ohno, T., Masaki, Y., Hirayama, S., Matsumura, M.: TiO₂-photocatalyzed epoxidation of 1-decene by H₂O₂ under visible light. *J. Catal.* **204**, 163–168 (2001)
19. Li, X., Chen, C., Zhao, J.: Mechanism of photodecomposition of H₂O₂ on TiO₂ surfaces under visible light irradiation. *Langmuir.* **17**, 4118–4122 (2001)
20. Kormann, C., Bahnemann, D.W., Hoffmann, M.: Photocatalytic production of H₂O₂ and organic peroxides in aqueous suspensions of TiO₂, ZnO, and desert sand. *Environ. Sci. Technol.* **22**, 798–806 (1988)
21. Coronado, J.M., Maria, A.J., Conesa, J.C., Yeung, K.L., Augugliaro, V., Soria, J.: EPR study of the surface characteristics of nanostructured TiO₂ under UV irradiation. *Langmuir.* **17**, 5368–5374 (2001)
22. Nakamura, R., Imanishi, A., Murakoshi, K., Nakato, Y.: In situ FTIR studies of primary intermediates of photocatalytic reactions on nanocrystalline TiO₂ films in contact with aqueous solutions. *J. Am. Chem. Soc.* **125**, 7443–7450 (2003)
23. Ikeda, S., Sugiyama, N., Murakami, S.-y., Kominami, H., Kera, Y., Noguchi, H., Uosaki, K., Torimoto, T., Ohtani, B.: Quantitative analysis of defective sites in titanium(IV) oxide photocatalyst powders. *Phys. Chem. Chem. Phys.* **5**, 778–783 (2003)
24. Nitta, A., Takase, M., Takashima, M., Murakami, N., Ohtani, B.: A fingerprint of metal-oxide powders: energy-resolved distribution of electron traps. *Chem. Commun.* **52**, 12096–12099 (2016)
25. Nitta, A., Takashima, M., Murakami, N., Takase, M., Ohtani, B.: Reversed double-beam photoacoustic spectroscopy of metal-oxide powders for estimation of their energy-resolved distribution of electron traps and electronic-band structure. *Electrochim. Acta.* **264**, 83–90 (2018)
26. Nitta, A., Takashima, M., Takase, M., Ohtani, B.: Identification and characterization of titania photocatalyst powders using their energy-resolved distribution of electron traps as a fingerprint. *Catal. Today.* **321–322**, 2–8 (2019)
27. Ohtani, B., Nitta, A., Takase, M., Takashima, M.: Identification and detailed characterization of metal oxide powders as a fundamental chemical Pproduct. *KnE Soc. Sci.*, 787–795 (2019). <https://doi.org/10.18502/kss.v3i18.4768>
28. Abe, R., Takami, H., Murakami, N., Ohtani, B.: Pristine simple oxide photocatalysts as visible light driven photocatalysts: highly efficient decomposition of organic compounds over platinum-loaded tungsten oxide. *J. Am. Chem. Soc.* **130**(25), 7780–7781 (2008)
29. Murakami, N., Abe, R., Prieto-Mahaney, O.-O., Torimoto, T., Ohtani, B.: Photoacoustic spectroscopic estimation of electron mobility in titanium(IV) oxide photocatalysts. *Stud. Surf. Sci. Catal.* **172**, 429–432 (2007)
30. Prieto-Mahaney, O.-O., Murakami, N., Abe, R., Ohtani, B.: Correlation between photocatalytic activities and structural and physical properties of titanium(IV) oxide powders. *Chem. Lett.* **38**(3), 238–239 (2009)
31. Ohtani, B., Prieto-Mahaney, O.-O., Amano, F., Murakami, N., Abe, R.: What are titania photocatalysts?—an exploratory correlation of photocatalytic activity with structural and physical properties. *J. Adv. Oxidat. Tech.* **13**(3), 247–261 (2010)
32. Murakami, N., Abe, R., Ohtani, B.: In-situ observation of photocatalytic reaction by photoacoustic spectroscopy: detection of heat of exothermic photocatalytic reaction. *Chem. Phys. Lett.* **416**, 316–320 (2008)



Professor Ohtani has been studying photocatalysis since 1981 and published ca. 300 original papers (h-index: 66). After gaining Ph. D. from Kyoto University in 1985, he became an assistant professor in the university, an associate professor in Graduate School of Science, Hokkaido University in 1996 and then a full professor in Institute for Catalysis, Hokkaido University in 1998.